

Research Article

Mechanical and Water Absorption Characterization of Mango Seed Shell/Epoxy Composite for Low Load Carrying Structures

K. Mohan Kumar ^{1,2,3,4} **Venkatesh Naik** ² **Sunil S. Waddar** ¹ **N. Santhosh** ¹
Vijayanand Kaup ² and **H. V. Harish** ⁵

¹Department of Mechanical Engineering, MVJ College of Engineering, Bangalore, 560067 Karnataka, India

²Department of Mechanical Engineering, CMR Institute of Technology, Bangalore, 560037 Karnataka, India

³Department of Mechanical Engineering, Research Scholar, Visvesvaraya Technological University, Jnana Sangama, Belagavi, Karnataka, India

⁴Research Center - Department of Mechanical Engineering, CMR Institute of Technology, Bangalore - 560 037, Affiliated to Visvesvaraya Technological University, Belagavi, Karnataka, India

⁵Department of Mechanical Engineering, Debre Markos University, Debre Markos, Gozamn, Misrak Gojam, Amhara, Zipcode 269, Ethiopia

Correspondence should be addressed to K. Mohan Kumar; mohankumark2019@gmail.com and H. V. Harish; harish_hv@dmu.edu.et

Received 23 December 2022; Revised 27 January 2023; Accepted 3 February 2023; Published 6 March 2023

Academic Editor: Chenggao Li

Copyright © 2023 K. Mohan Kumar et al. This is an open access article distributed under the Creative Commons Attribution License, which permits unrestricted use, distribution, and reproduction in any medium, provided the original work is properly cited.

The present work deals with the characterization of mango seed shell fiber reinforced epoxy composites by using hand layup method by varying the volume composition of the mango seed shell from 0 vol. % to 60 vol. % (M-0 to M-60). The physical density test, tensile test, flexural test, and water absorption test were conducted as per the American Society for Testing and Materials (ASTM) standards. Results revealed that the tensile strength of M-20 (20 vol. %) is 43% more than a neat epoxy, while the flexural strength of M-50 (50 vol. %) is greater than 10.85% more than a neat epoxy. The water absorption test was conducted by immersing the samples in distilled water at room temperature, and the weight of the specimens was measured and recorded at every 24-hour time interval. For all composite samples, saturation in water absorption and thickness swelling were observed after 432 hours of water immersion. The moisture absorption increases with the inclusion of reinforcements as compared to the neat epoxy samples. However, for the M-50 composite, the water absorption decreases due to the uniform mixing and stronger bonding between the matrix and the reinforcements. The scanning electron microscope (SEM) images of the composite specimens also depicted the particulate fiber distribution and the presence of micro-voids in the epoxy matrix.

1. Introduction

The need for novel biocompatible and sustainable reinforcements has triggered interests in the research community to explore non-traditional sources of reinforcements from non-edible agricultural sources. In this regard, the use of mango seed shell in thermoset polymers is a unique work that has the potential to become an alternative to the conventional synthetic reinforcements and resin-based polymer composites.

The choice of matrix material is also important for the synthesis of the natural reinforcement-based polymer composites,

and among the resin materials, thermoset polymers have several applications particularly with grounded particles and flakes, especially when mixed or moulded with varying volumetric ratios of the fiber/fiber particles, as in epoxy resin, polymer, and phenolic polyamide resins. Several studies have been done on thermosetting composites [1] with the incorporation of particulates of prawn shells, tamarind, and dates seed powders along with *Arundo Donax* L. leaf, which are used as reinforcement in the epoxy resin matrix [2]. The research on natural filler-based thermoplastics is still in its incipient stage, and there is a vast scope carrying out the synthesis and



FIGURE 1: (a) Particulate form of mango seed shell. (b) Epoxy resin and hardener used for composite preparation.

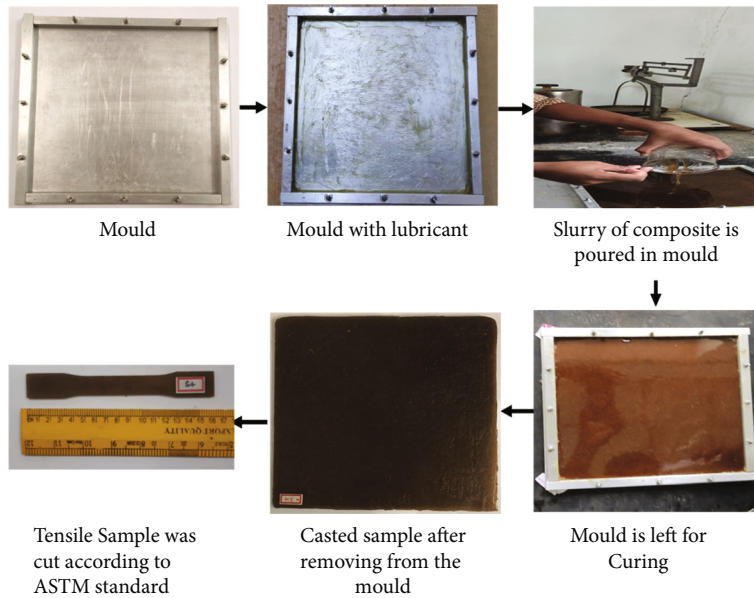


FIGURE 2: Composite fabrication flowchart.

TABLE 1: Volume ratio of different constituents of the composite specimens prepared.

Designation	Vol. % of mango seed shell	Vol. % of resin	Vol. % of hardener
M-0	0	66.67	33.33
M-10	10	60	30
M-20	20	53.33	27.67
M-30	30	46.67	23.33
M-40	40	40	20
M-50	50	33.33	16.67
M-60	60	26.67	13.33

characterization of these composites. As demonstrated by various researchers through their theoretical and experimental investigations, the natural filler-based materials are known to enhance the mechanical characteristics of the composites.

Mechanical properties such as tensile, impact, and flexural strength are observed to increase, when palm fiber and tamarind seed paste are used as reinforcements in the epoxy resin [3]. The composites are synthesized using randomly dispersed groundnut shell particles of various grain sizes and an epoxy resin matrix, and it is discovered that grain size has a significant influence on the mechanical characteristics of the composite, viz., the tensile and impact strength characteristics [4]. Epoxy-based hybrid composites are produced by reinforcing areca and coconut shell powder, and the cast composite is tested for density, void content, and thermal characteristics according to American Society for Testing and Materials (ASTM) standards [5]. Further, luffa cylindrical is used as the reinforcement, epoxy resin as the matrix with furfural alcohol, and NaOH for the surface treatment of the reinforcements, which resulted in improved mechanical characteristics [6]. Silane treatment is applied to a composite with the luffa cylindrical as reinforcement and epoxy LY556 as matrix. The

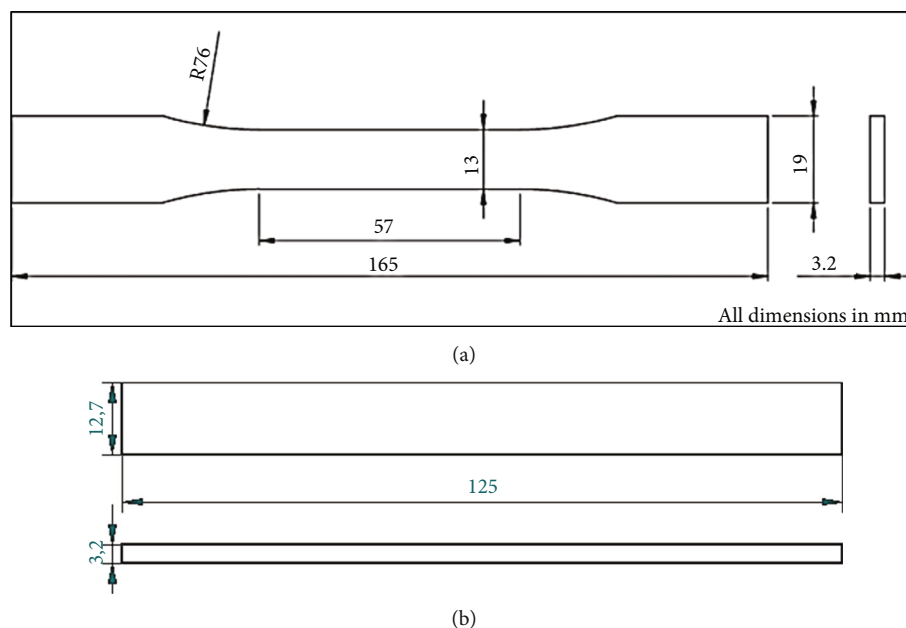


FIGURE 3: (a) Tensile test specimen used in the present work (ASTM D638-TYPE 2 standard dimensions). (b) Flexural test specimen used in the present work (ASTM D790 standard dimensions).

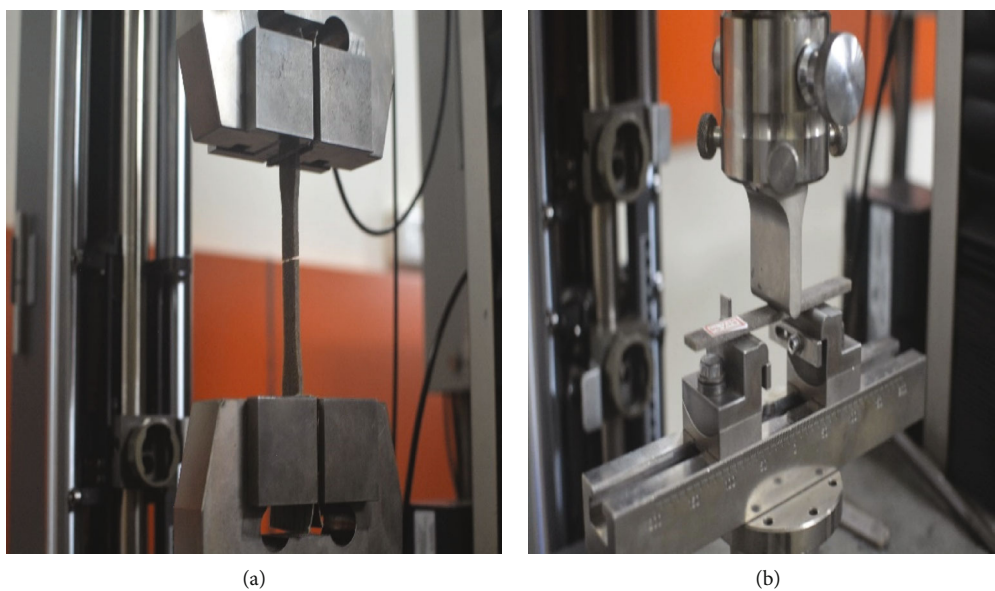


FIGURE 4: (a) Specimen loaded in tensile test. (b) Specimen loaded in three-point bending flexural test.

composite is cast using the hand-layup method and evaluated according to ASTM standards for flexural properties [7]. The matrix material is the combination of epoxy (LY-5082) and hardener (HY-5082), and the reinforcement is luffa cylindrica. After alkali treatment, the composite is cast using compression moulding, and mechanical tests such as tensile and flexural are performed. It is herewith reported that the tensile and flexural characteristics of the composites improve with the inclusion of natural filler in the matrix phase [8]. Polyalthia longifolia seeds (mast tree seed/Ashoka tree) are finely ground and used as reinforcement, with Vinyl ester serving as the matrix. The composite is cast using compression

moulding, and mechanical tests such as tensile, impact, and flexural are performed. The results show that the properties of the composites improve with the inclusion of natural filler in the matrix [9]. Ground nut shells and coconut coir are used to make a composite, with Araldite LY-556 as the matrix material and HY-951 as the hardener. The fibers used are in particulate form, and mechanical tests such as tensile and flexural are performed. It is herewith reported that the characteristics of the composites improve with the inclusion of natural fillers in the matrix [10]. The resin is cured at room temperature with the addition of a cobalt accelerator and Methyl Ethyl Ketone Peroxide (MEKP) catalyst. Okra fibers

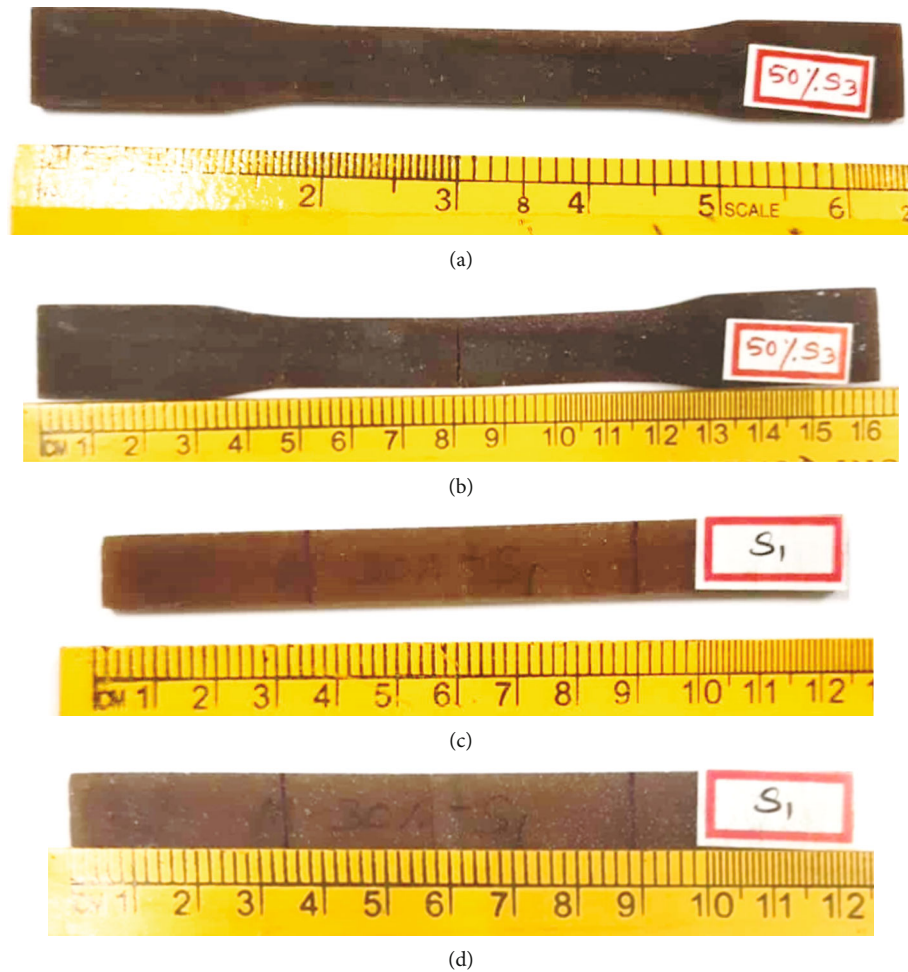


FIGURE 5: (a) Tensile specimen before testing. (b) Tensile specimen after testing. (c) Flexural specimen before testing. (d) Flexural specimen after testing.



FIGURE 6: Samples immersed in distilled water.

are utilized as reinforcements. The results reveal that the inclusion of okra fibers along with cobalt accelerator and MEKP catalyst provides greater strength in comparison with the neat epoxy [11]. Jack fruit skin powders are used as reinforcements and polylactic acid (PLA) as the matrix material for the composite that is fabricated by hot press/compression moulding [12], while melon shell particles are used as reinforcement and epoxy LY556 resin and HY951 hardener are used as matrix and the composite is fabricated using hand-layup method, also they are post-processed using carbonizing [13]. Composite is cast using compression moulding where fish scales are used as reinforcement followed by epoxy LY556 as the matrix phase. It is herewith reported from the research findings that the cast composites exhibit better characteristics due to the inclusion of fillers in the matrix in comparison with the neat epoxies [14]. Tamarind seed powders and coconut seed powders are used as reinforcements followed by epoxy resin as the matrix. The composites are produced by hot press/compression moulding [15], [16]. The sustainability and strength characteristics of the composites are enhanced by the inclusion of fillers in the matrix and are ascertained from the findings of the several other

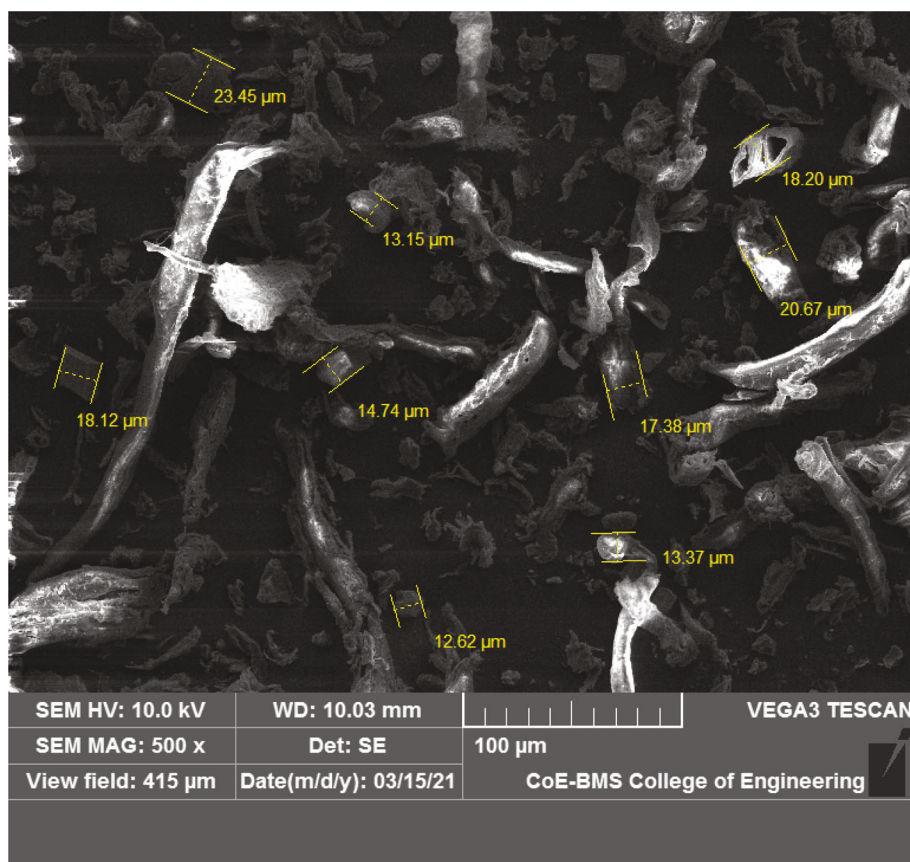


FIGURE 7: SEM image of mango seed shell powder.

TABLE 2: Theoretical and experimental densities of prepared composites.

Sl. no.	Sample type	Theoretical density	Experimental density	Void content	% weight reduction
1	M-0	1190.00	1190.00 ± 14.28	—	—
2	M-10	1184.42	1167.72 ± 16.11	1.41	1.87
3	M-20	1178.84	1166.67 ± 17.27	1.03	1.96
4	M-30	1173.26	1157.16 ± 17.59	1.37	2.76
5	M-40	1167.68	1127.98 ± 31.58	3.40	5.21
6	M-50	1162.10	1157.41 ± 32.41	0.40	2.74
7	M-60	1156.52	1116.67 ± 34.62	3.45	6.16

researchers [17–21]. The strength and toughness of the polymer composites are enhanced by strong bonding between the matrix and the reinforcements, and also the molecular adhesion between the resin and fibers is enhanced by the filler materials that inoculate and create a stronger bond, thereby inhibiting the water uptake by the composites [22–28]. This serves as the major reason for using the mango seed shell as reinforcements in the matrix to improve the mechanical characteristics and reduce the moisture absorption by the composites.

The present work focuses on the study of mechanical properties such as the density, tensile properties, flexural properties, and water absorption properties of epoxy resin (LAPOX L-12), K6 hardener, and finely ground mango seed

shell particulate fiber reinforced composites, which has substantial novelty in the very fact that the mechanical properties are critically analyzed and mapped with respect to the ability of mango seed shell to absorb moisture content and the presence of voids in the composite. The research on mango seed shell particulates is still in its incipient stage and there is a vast scope for accomplishing further research in this domain. Also, the epoxy resin-based composites with optimum volume percentage of the dried mango shell powder can be used for structural applications, especially for those structures requiring higher strength to lower volumes, viz., the automobile bumpers, dashboards, panels, and seat structures, etc. The non-traditional variety of natural reinforcements from discernable waste sources, viz., the mango seed shell, can be effectively used as reinforcements for eco-compatible composites.

2. Materials and Methods

2.1. Materials. In this study, the finely grinded mango endocarp seed particulate is used as reinforcement. The mango seed is a single, flat, oblong seed that may have fibrous or hairy surface. Totapuri mango (or Ginimoothi) of *Mangifera* genus and *Mangifera indica* species, which is cultivated in Karnataka, India, is used in current work, which is a single embryo about 4–7 cm long, 3–4 cm wide, and 1 cm thick and is housed inside the seed coat, which is 1–2 mm thick.

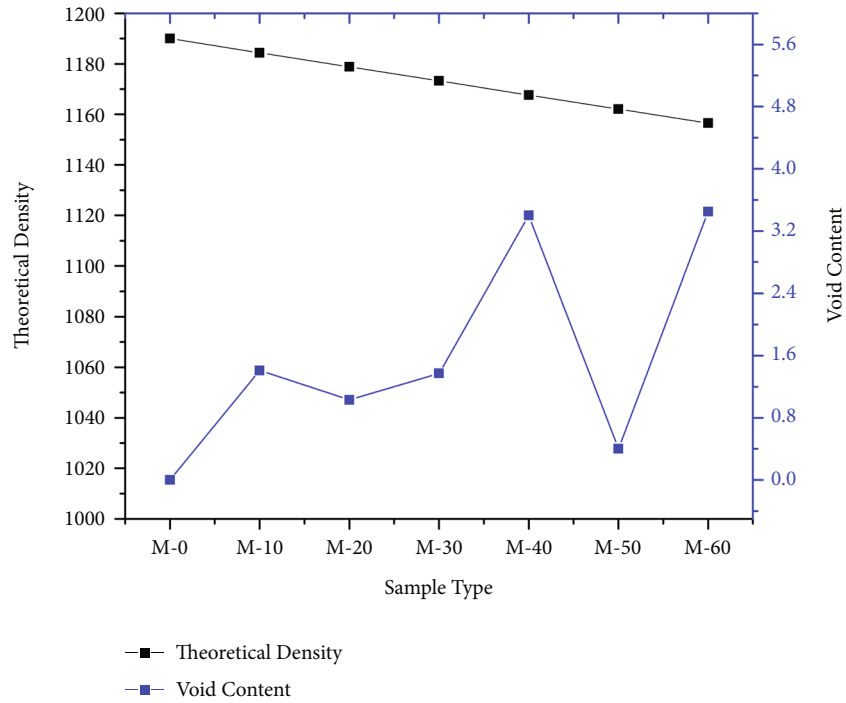


FIGURE 8: Theoretical density and void content of different sample types.

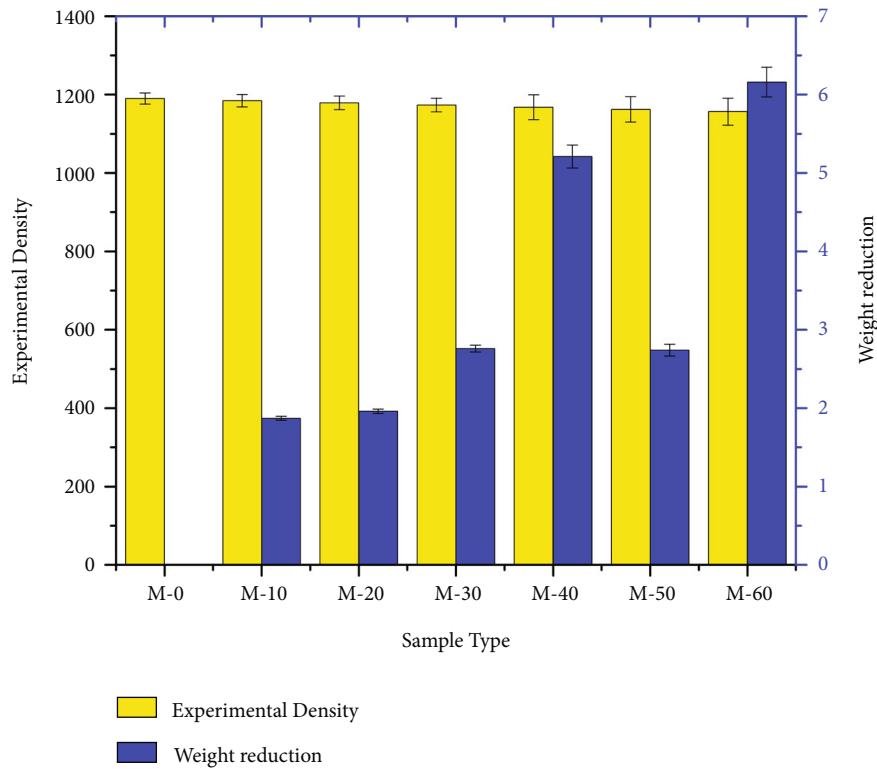


FIGURE 9: Experimental density and weight reduction for different sample types.

The extraction method of mango seed shell in powder form for the manufacturing of epoxy-based composites is a critical technique. The mango seeds are collected from juice making industry and then dried in sunlight for 7 days. The shells of the mango seeds are taken and cleaned with distilled water

and dried in bright sunlight for 2 days. The flexibility in the shell wall is checked manually and later the NaOH solution and dried in bright sunlight for 2 days. The flexibility in the shell wall is checked manually and is heated until the solution boils for a duration of 20 minutes, so that dust, dirt,

TABLE 3: Tensile properties of mango seed shell/epoxy composites.

Sl. no.	Sample type	Tensile modulus (MPa)	Tensile strength (MPa)	Strain (%)
1	M-0	368.43 ± 105.97	20.98 ± 1.75	2.047
2	M-10	233.55 ± 36.79	28.73 ± 9.70	3.044
3	M-20	276.43 ± 84.50	30.02 ± 1.28	3.970
4	M-30	235.50 ± 102.86	12.10 ± 4.05	3.538
5	M-40	302.52 ± 106.99	13.25 ± 1.68	2.450
6	M-50	254.55 ± 44.34	22.56 ± 6.84	2.885
7	M-60	250.01 ± 58.09	17.32 ± 1.91	2.574

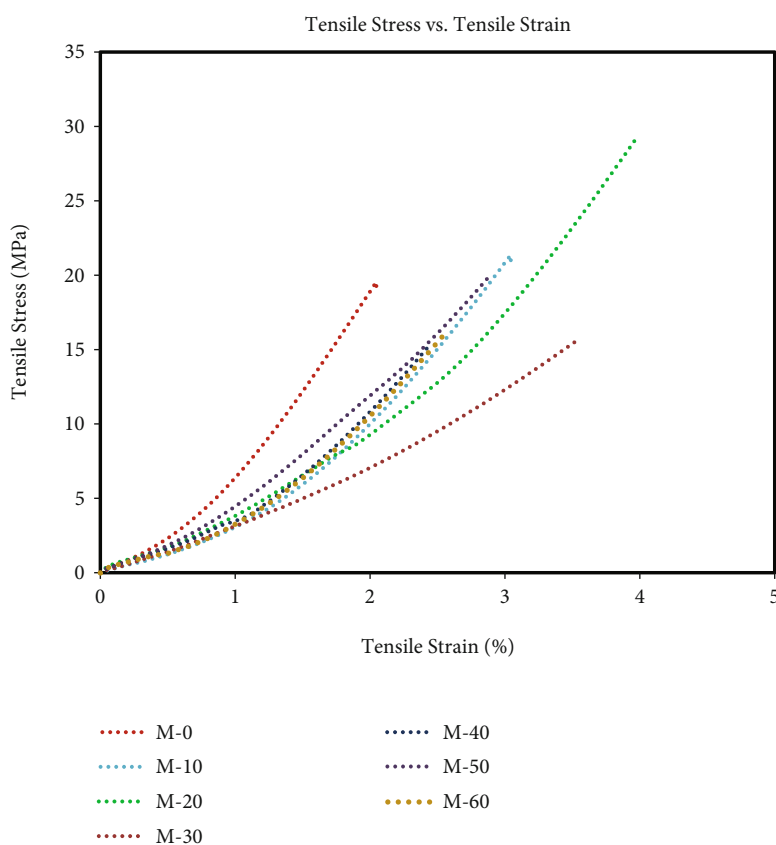


FIGURE 10: Stress–strain diagram for different composite specimens.

and lignin content onto surface are removed. Later the NaOH solution is cooled in room temperature, the shells are separated and dried in sunlight for 2 days. The dried shells are further kept in oven at a temperature of 50°C for 1 hour to remove the moisture content. The dried shells are grinded using the domestic grinder to convert into powder form. The powder is sieved using $75\mu\text{m}$ sieve. This mango seed shell powder is used as the reinforcement in epoxy matrix. Figure 1(a) gives the photograph of the particulate form of mango seed shell used in the present work.

The combination of LAPOX L-12 epoxy resin with K6 hardener is used as matrix. The resin and hardener are procured from Yuje Enterprises, Bengaluru, India (Figure 1(b)). Lapox L-12 is a liquid, unmodified epoxy resin of medium viscosity used with various hardeners for making compos-

ites. The Lapox L-12 resin has a density in the range of $1.12\text{--}1.19\text{g/cm}^3$, dynamic viscosity in the range of $50\text{--}95\text{MPa s}$, flash point greater 200°C , and storage temperature in the range of $2\text{--}40^{\circ}\text{C}$ as per the technical specification datasheet provided by the supplier.

The use of the non-edible discernable agricultural wastes as reinforcements for the composites is supported by some of the research findings similar to the present work. N. P. Sunesh et al. [29] have worked on the novel agrowaste-based cellulosic micro-fillers from *Borassus flabellifer* flower for polymer composite reinforcement. The results have showed that an agricultural residue can be converted into a valuable micro-sized cellulosic filler material for polymeric composite applications that can withstand processing temperature up to 200°C .

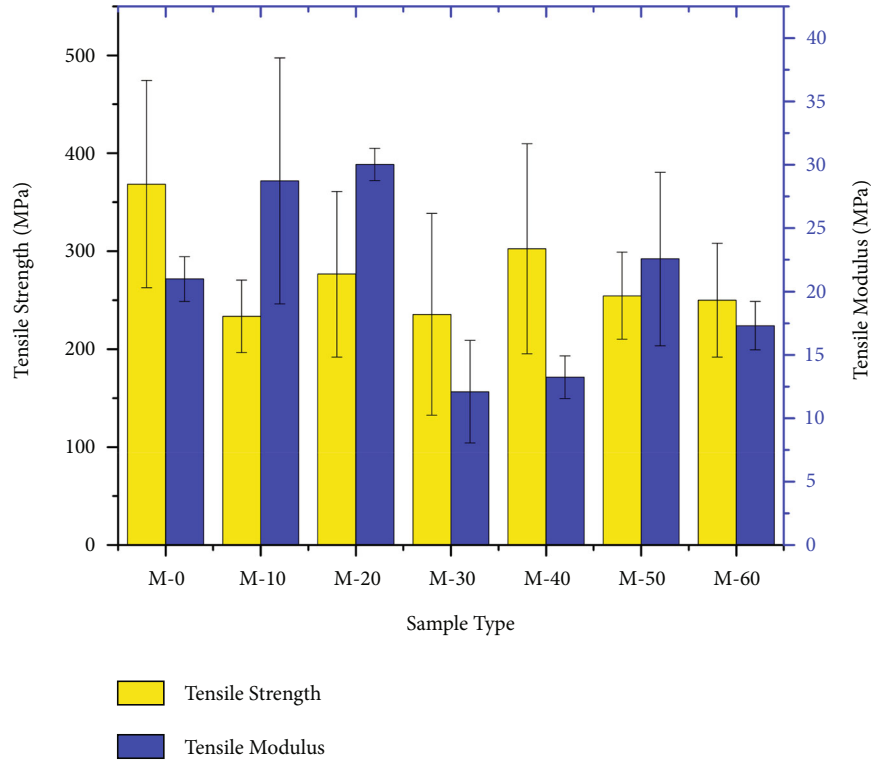


FIGURE 11: Tensile strength and tensile modulus for mango seed shell/epoxy composites.

2.2. Sample Preparations. In the present work, the composites are prepared by manual stir casting method by homogeneously mixing mango seed shell particulate (powdered form) in epoxy matrix medium. For this work, an aluminium mould of size $240\text{ mm} \times 240\text{ mm} \times 4\text{ mm}$ is fabricated, and is as shown in Figure 2. Initially, the silicone releasing agent is applied to mould for easy removal of casted samples. At room temperature, a required volume percent of mango seed shell particles is mixed with epoxy resin (Lapox L-12) and K6 hardener mixture prepared in the volumetric ratio of 2:1 and then poured into the mould. Table 1 gives the volume ratio of different constituents of the composite specimens prepared in the present work. After casting, the composites are subject to hot air blower drying before curing to remove the entrapped moisture, water vapour bubbles from the composite specimens. The hot air blower dried cast slabs are then cured at room temperature for 24 hours. Subsequently the moisture check is accomplished by gravimetric test method in accordance with ASTM D5229 test standards. There are distinct particulate composites that are synthesized, by varying the mango particles concentration in the range of 10%–60% by volume in an epoxy matrix. The specimens are cut from the composite slabs for different tests as per the ASTM standards. The flow chart of composite fabrication is given in Figure 2.

2.3. Material Characterization

2.3.1. Density and Void Contents Measurement. According to ASTM 792-20 standard, the procedure to measure the densities of mango seed shell/epoxy composites with sample

size $50 \times 10 \times 4\text{ mm}$ were used for density measurement. Here, the medium used for density is distilled water. The mass of the specimen in air and in water was measured using a digital weighing scale with 0.001 grams resolution.

Based on Equation (1), the composite density is calculated,

$$\rho_{\text{exp}} = \frac{M_a}{M_a - M_b} \times 1000, \quad (1)$$

where ρ_{exp} is the composite density, M_a is the mass of specimen in air, and M_b is the mass of specimen in distilled water. For each case, three specimens have been checked and the average value is taken into account.

Void content is the term used to describe the air trapped during the manual mixing of mango seed shell in epoxy. By taking into consideration, the relative discrepancy between the theoretical and experimentally determined densities, the void content of the composite is calculated.

ASTM D2734-16 test procedure is followed to determine the void content. The percentage void content was calculated based on the given Equation (2),

$$v_c = \frac{\rho_{\text{th}} - \rho_{\text{exp}}}{\rho_{\text{th}}} \times 100, \quad (2)$$

where v_c is the percentage of void content, ρ_{th} is the theoretical composite density, and ρ_{exp} is the experimental composite density.

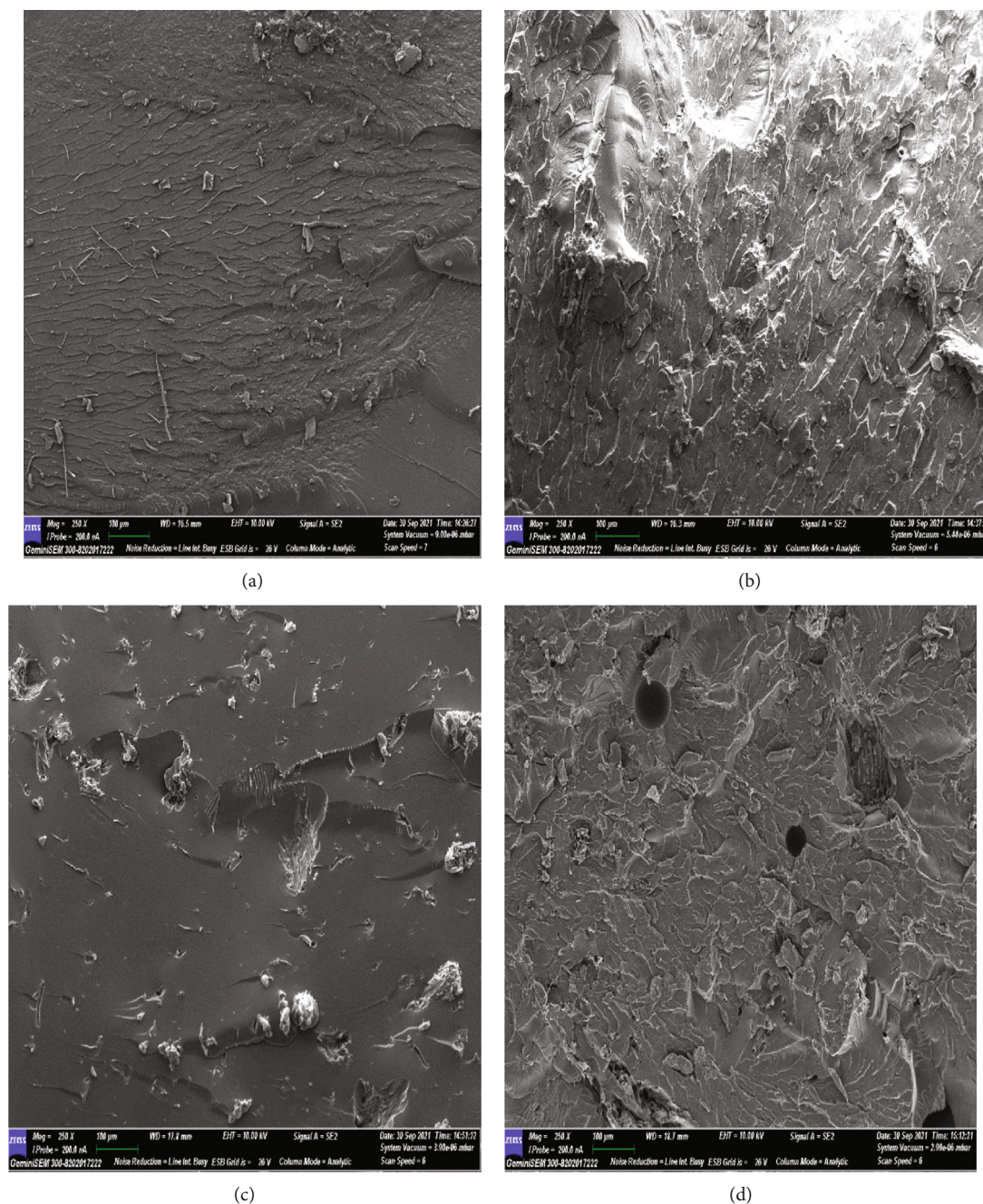


FIGURE 12: SEM images of tensile test failed composite surfaces for (a) M-0, (b) M-20, (c) M-40, and (d) M-60.

2.3.2. Mechanical Testing. All mechanical testing were carried out in accordance with ASTM standards. The tensile and three-point bending tests were performed using a Zwick-Roell universal testing machine with a load cell capacity of 20 kN, model Z020, according to ASTM D 3039-00 and ASTM D 7264-07 test procedures, respectively, with a cross head travel speed of 2mm/min. For the flexural test, the span to thickness ratio of the test sample was maintained at 32:1. Four samples were tested for each case and average values considered. Figures 3(a) and 3(b) give the dimensions of the flexural and tensile test specimen, while Figures 4(a) and 4(b) and give the

photograph of specimen loaded in tensile test and three-point bending flexural test.

The Figure 5(a) gives the photograph of the tensile specimen before testing, while Figure 5(b) gives the photograph of the tensile specimen after testing, while Figure 5(c) gives the flexural specimen before testing, while Figure 5(d) gives the photograph of the flexural specimen after testing. The photographs clearly depict the fracture that has occurred in the tensile and flexural tests.

2.3.3. Water Absorption. The mango seed shell/epoxy composites water absorption behavior was investigated in

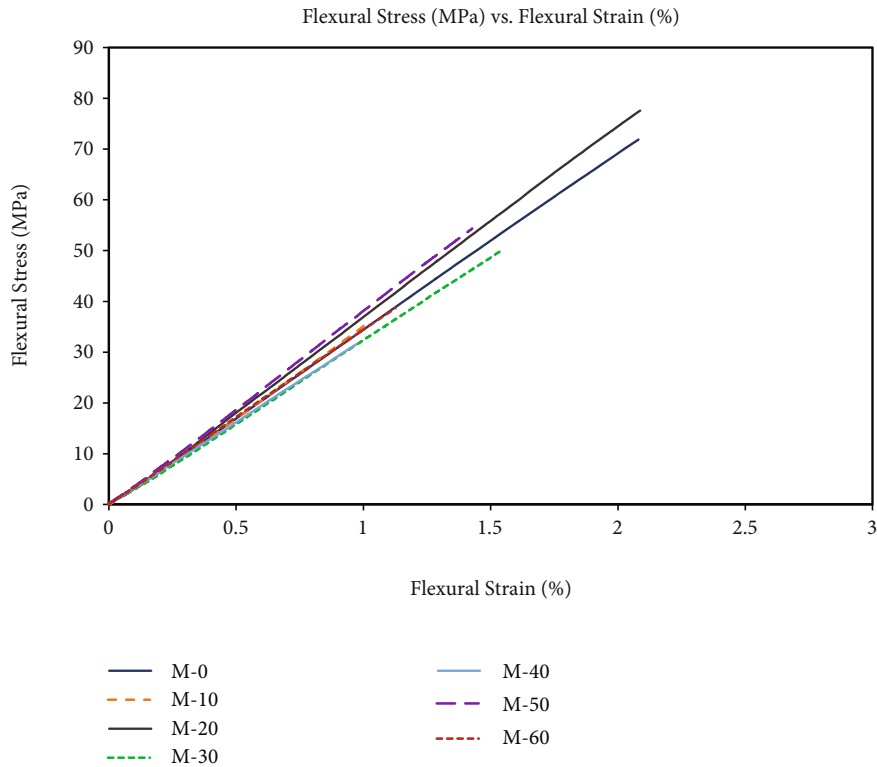


FIGURE 13: Flexural stress vs. strain for different composite specimens.

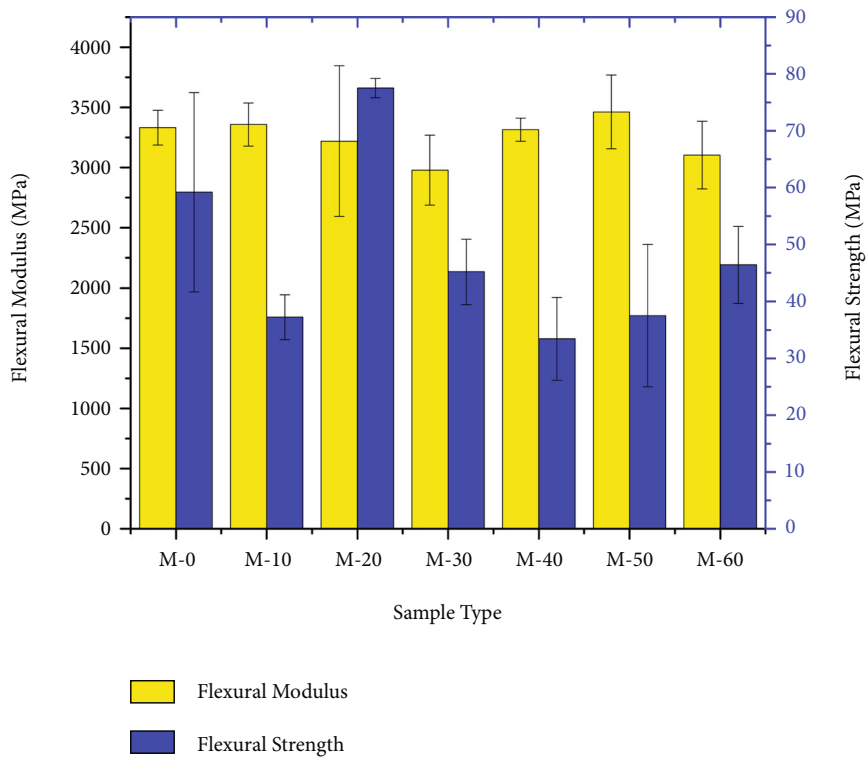


FIGURE 14: A representative graph for flexural strength and flexural modulus for mango seed shell/epoxy composites.

accordance with ASTM D570-98 standard. For this study, samples with dimensions of 75 mm × 25 mm × 4 mm were employed. The samples were dried for 2 hours at 70°C in

an oven before being chilled in a desiccator and as soon as they reach room temperature, their original weight (M_r) was recorded using laboratory weighing balance. Later, the

TABLE 4: Flexural properties of mango seed shell/epoxy composites.

Sl. no.	Sample type	Flexural modulus (MPa)	Flexural strength (MPa)	Flexural strain (%)
1	M-0	3330.74 ± 144.71	59.20 ± 17.51	2.080
2	M-10	3356.90 ± 178.50	37.24 ± 3.93	1.024
3	M-20	3218.82 ± 626.20	77.50 ± 1.72	2.087
4	M-30	2977.98 ± 290.41	45.19 ± 5.73	1.549
5	M-40	3313.78 ± 96.48	33.44 ± 7.30	0.973
6	M-50	3462.26 ± 307.25	37.50 ± 12.51	1.427
7	M-60	3104.03 ± 281.07	46.40 ± 6.74	1.126

samples were then entirely immersed in distilled water. The samples were removed from the distilled water at every 24-hour interval, the surface water was quickly wiped with tissue paper, and their weight (M_t) was recorded within 30 seconds. This process was continued until an equilibrium condition was attained. For each case, three samples were examined. Figure 6 gives the photograph of the samples immersed in the distilled water.

The weight gain reveals how much water is being absorbed. The percentage of water absorption was obtained using Equation (3),

$$W_a = \frac{M_t - M_r}{M_t} \times 100. \quad (3)$$

According to ASTM D 570-98 standard, the thickness swelling behavior of mango seed shell/epoxy composites was investigated. The thickness swelling test was conducted using the identical water absorption test samples. Using a digital Vernier caliper, sample thickness was additionally recorded each time along with weight. The percentage thickness swelling was calculated using Equation (4),

$$T_s = \frac{T_t - T_r}{T_t} \times 100, \quad (4)$$

where T_t and T_r are the thickness of dried sample and the sample after immersion in water for time T_s , respectively.

2.3.4. Morphological Analysis. A scanning electron microscope (SEM) HR-FESEM (GEMINI 300, Carl Zeiss, Germany) is used to examine microstructure. Prior to analysis, each sample is sputter coated using a JFC-1600 auto fine coater (JEOL, Japan) and studied for the morphological features.

3. Results and Discussions

3.1. Characterization of Mango Endocarp Seed Particulate. In this work, the mango seed was collected from the Sunsip Agro Processor factory, which makes mango sip juice in Srinivaspur Taluk, Kolar District, Karnataka. Then the mango seed endocarp was dried and finely ground. The morphology of the mango seed shell powder is fibrous flaky type, with the diameter of the flakes and particulates varying in the range

of 12–25 μm . The SEM image of the mango seed shell is shown in Figure 7.

3.2. Density and Void Contents. Table 2 presents theoretical and experimental densities of mango seed shell/epoxy composites. Density of mango seed shell/epoxy composites decreases in the range of 1.87–6.16% with increasing filler content as compared to neat epoxy.

Void content increases in a narrow range of 1.41–3.45 with higher mango seed shell loadings as observed from the graph in Figure 8. Lower void contents signify consistency in processing route and good quality of the samples.

The porosity is having a greater impact on the mechanical characteristics of the composite samples, and the porosity can be reduced by accomplishing the fabrication of the composite laminates in vacuum and uniformly rolling the laminate in the die to remove the entrapped air and water bubbles.

The Figure 9 gives the comparative representation of experimental density and weight reduction for different sample types and thereby provides an overview of the effect of void content on the density and % weight reduction of the composite specimens. The void content as well as the % weight reduction are maximum for M60 composite specimen. However, the strength decreases with the void concentration.

3.3. Materials Characterizations

3.3.1. Tensile Properties. The tensile strengths were higher for higher volume fractions of the mango seed shell powder, while the tensile modulus was higher for lower volume fractions and lower for higher volume fractions, as shown in Table 3, which displays the mechanical characteristics of mango seed shell/epoxy composites. The observed behavior is likely to persist because the reinforcements are dispersed randomly and since tensile strength is a property that depends on direction. Figure 6 shows the response of the material tensile strength and tensile modulus of mango seed shell/epoxy composites. It shows that M-20 with 30.02 ± 1.28 MPa possess the maximum tensile strength and M-40 with 13.25 ± 1.68 MPa possess the minimum tensile strength and M-20 depicts a 43.06% increase in tensile strength compared with pure epoxy laminate. Similarly, it shows that M-40 with 302.52 ± 106.99 MPa possess the maximum tensile modulus and M-10 with 233.55 ± 36.79 MPa possess the minimum tensile modulus. Table 3 displays the mechanical characteristics of mango seed shell/epoxy composites, while the Figure 10 gives the stress-strain diagram for different composite specimens.

From Figure 10, it is evident that the tangent modulus increases with the increase in the stress, depicting the semi-elastic action of a material when subjected to excessive stress. Thus, the inclusion of optimum vol. % of mango seed increases the slope of the linear region of the stress-strain curve, thereby improving the tensile characteristics of the composite. The findings are supported by the literature of similar works carried out by P. J. Herrera-Franco et al. [30], wherein the elastic modulus, in the longitudinal

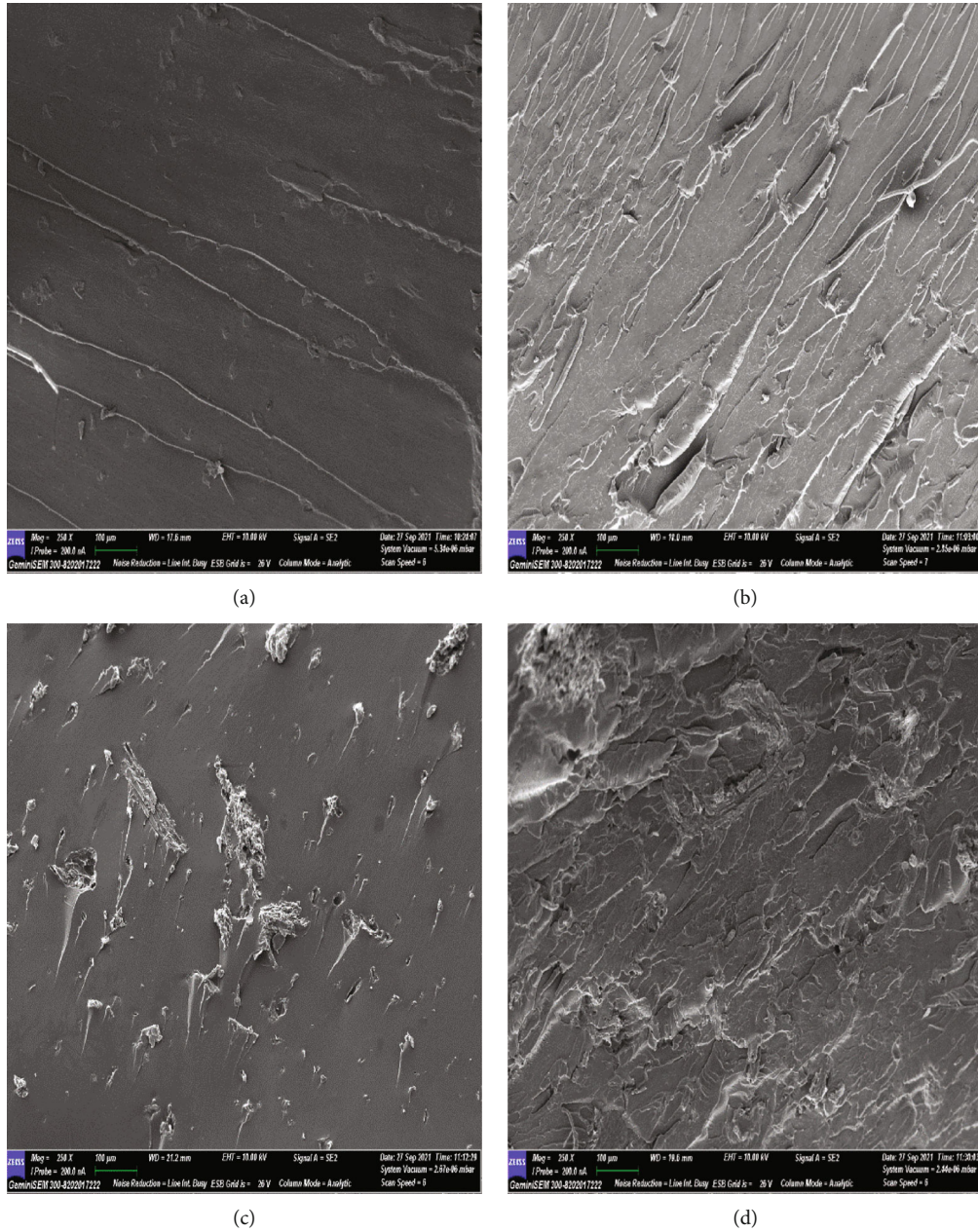


FIGURE 15: SEM images of flexural test failed composite surfaces for (a) M-0, (b) M-20, (c) M-40, and (d) M-60.

direction of the reinforcements, obtained from the tensile and flexural measurements as compared to the values calculated using the rule of mixtures showed a remarkable improvement. The increase in the mechanical properties ranged between 3% and 43%, for the longitudinal tensile and flexural properties, whereas in the transverse direction to the reinforcements, the increase in the mechanical properties, viz., the tensile and flexural, ranged between 5% and 50%. This improvement is attributed to the fact that, with the increasing reinforcement-matrix interaction, the failure mode changed from interfacial failure to matrix failure and the inclusion of the natural reinforcements from seed carps of monoembryonic kernel seed sources tend to improve the tensile properties of the composites. Figure 11 gives the

representative graph for tensile strength and tensile modulus for mango seed shell/epoxy composites.

The matrix and reinforcement possess stronger bonding and exhibit better strength characteristics. Figure 12(a) clearly shows no matrix deformation near the breakage zone in the M-0 composite, thereby indicating a stronger interstitial atomic bonding between the resin and hardener in the matrix phase. Figure 12(b) clearly shows that there is substantial matrix deformation near the breakage zone in the M-20 composite, due to the fracture of the bonds owing to the peripheral growth of the particulates. Figure 12(c) clearly shows matrix deformation near the breakage in the M-40 composite, and the mango seed shell particulates, in matrix phase that are visible in the SEM micrograph, clearly depict

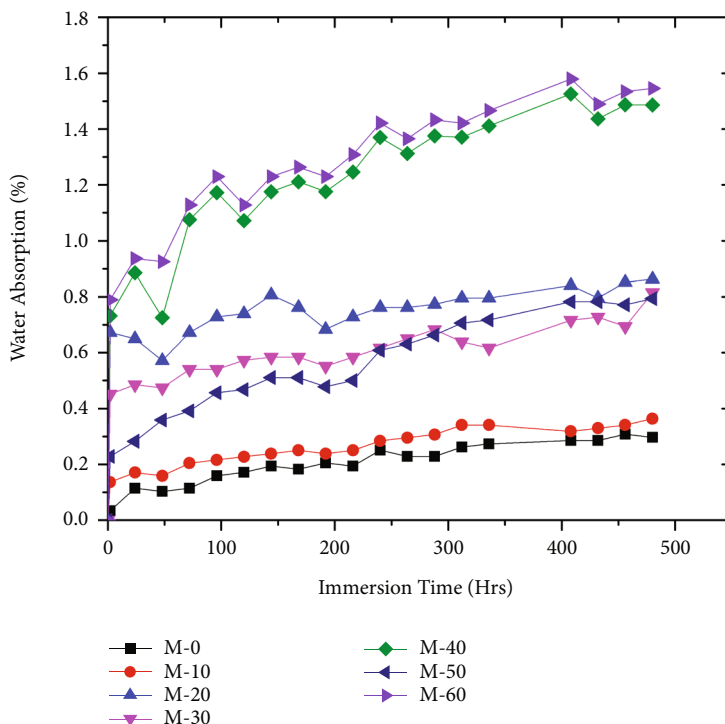


FIGURE 16: Water absorption behavior of mango seed shell/epoxy composites.

the strength of the interstitial bonding that leads to enhanced strength attributed to stronger adhesion between the matrix and the reinforcements. Figure 12(d) clearly shows there is severe matrix deformation near the breakage with void absorbed in the M-60 composite. Stronger adhesion between the particulates and the matrix is indicated by the fiber pull-out phenomena as is the case in the SEM image for M-40 composite.

3.3.2. Flexural Properties. The specimen under flexural force experiences both normal and shear stresses. The top portion of the test specimen experiences compressive stress during the flexural test, whereas the bottom portion experiences tensile stress. Figure 13 gives the flexural stress vs. strain for different composite specimens, while Figure 14 gives the response of the material flexural strength and flexural modulus of mango seed shell/epoxy composites. It shows that M-20 with 77.50 ± 1.72 MPa is the maximum flexural strength and M-40 with 33.44 ± 7.30 MPa is the minimum flexural strength and M-50 is having 10.85% decrease in flexural strength compared with pure epoxy laminates. Similarly, it shows that M-50 with 3462.26 ± 307.25 MPa is maximum flexural modulus and M-30 with 2977.98 ± 290.41 MPa is the minimum flexural modulus. Table 4 displays the flexural mechanical characteristics of mango seed shell/epoxy composites.

The matrix and reinforcement exhibit stronger bonding due to adhesive forces. Figure 15(a) clearly shows no matrix deformation near the breakage in the M-0 composite. Figure 15(b) clearly shows there is a greater matrix deformation near the breakage in the M-20 composite. Figure 15(c) clearly shows that there is moderate matrix deformation

near the breakage in the M-40 composite, while good adhesion between the fiber and matrix is indicated by the fiber pull-out phenomena. Figure 15(d) clearly shows that there is more matrix deformation near the breakage in the M-60 composite, due to the transfer of load to the reinforcement from the matrix.

The results of flexural strength and flexural modulus for the present work are in close correlation with the findings of Venkatesh Naik et al. [31], whose results have revealed that the flexural properties of the composites improve with the increase in the vol. % of mango seed shell up to an optimum composition.

3.4. Water Absorption. Figure 16 gives the water absorption behavior of mango seed shell/epoxy composites over a period of time. It is evident that all composite materials quickly absorb water during the first few minutes of immersion before gradually moving toward saturation over time. This behavior is seen in all the combinations of the composites synthesized in the present work. From the works of Kazi et al. [32], the same pattern of water absorption behavior for the natural composites is observed. The water absorption for neat laminate is the minimal in comparison with all the other combinations of the composites, followed by M-10 type of composite. Among the composites, as the volume percentage of mango seed shell reinforcement increases, the water absorption rate also increases. However, in case of M-40 and M-60 type of composite, the water absorption rate drastically increases owing to the presence of voids and porosity. The water absorption rate is maximum for M-60 composite, followed by M-40 type of composite. The water absorption rate for M-50 type composite is lesser than

that of M-20 type and M-30 type composite, due to the uniform rolling of the mixture in the mould leading to the removal of entrapped air and stronger bonding between the matrix and the reinforcement. The change in the water absorption rate for all the composites was observed to be predominant for the initial 18 days, post which the water uptake by composites almost reached its saturation.

The water absorption behavior of mango seed shell/epoxy composites is in line with the findings of Sekar Sanjeevi et al. [33] who have carried out investigation to understand the effects of water absorption on the mechanical properties of hybrid phenol formaldehyde (PF) composite fabricated with Areca Fine Fibers (AFFs) and Calotropis Gigantea Fiber (CGF). They have reported that the increase in the fiber content increased the water absorption; however, after 120 hours of immersion, all the composites attained an equilibrium state.

4. Conclusions

- (i) The density, tensile, flexural, and water absorption characteristics of the mango seed shell/epoxy composites have been investigated for different vol. % of the mango seed shell ranging from 0 vol. % to 60 vol. %.
- (ii) From the density tests and the comparison between the theoretical and experimental values, the void content for the specimens ranges from 1.41% to 3.45%, thereby ascertaining a relatively good quality for the composite specimens fabricated.
- (iii) The experimental findings further depict higher tensile strength for the composite specimens with the inclusion of mango seed shell powder reinforcements of up to 20 vol. % in comparison with the neat epoxy laminates with an increase in the tensile strength values by 43.06%. However, an increase in the reinforcement content beyond 20–30 vol. % and 40 vol. % reduces the tensile strength, attributed to the increase in the void content to about 3.40% in the composite, further increase in the composition of the reinforcements to 50 vol. % slightly improves the tensile strength by 7.54%, due to the reduction in the void content in the laminate attributed to the compaction of reinforcements in the matrix. But the increment in the vol. % of mango seed shell powder to 60 vol. % once again reduces the tensile strength by 17.47%.
- (iv) The results of flexural strength also depict more or less a similar trend, except for the 50 vol. % reinforcement with the flexural strength being maximum at 77.5 MPa (an improvement of 30.91%) for the composite specimen with 20 vol. % mango seed shell reinforcement.
- (v) The morphological analysis of the fractured surfaces of the composite specimens has revealed proof of resin de-bonding and pull-out of the reinforcement

particles, with the increase in the mango seed shell powder content attributed to inadequate load transfer between the matrix and the reinforcement content due to the increase in the void content. However, the strength of the composites can be increased with the reduction in the weight by reinforcing the epoxy resin with optimum content of the mango seed shell powder and proper compaction.

- (vi) The results of the water absorption test have revealed that the saturation in water absorption and thickness swelling is observed only after 432 hours of water immersion. The moisture absorption increases with the inclusion of reinforcements as compared to the neat epoxy samples. However, for the M-50 composite, the water absorption decreases due to the uniform mixing and stronger bonding between the matrix and the reinforcements. Thus, the epoxy resin-based composites with optimum volume percentage of the dried mango shell powder reduces the water absorption by the composites.

Data Availability

The datasets used in the manuscript is readily available and will be furnished upon request.

Conflicts of Interest

The authors declare that they have no conflicts of interest.

Acknowledgments

The authors would like to thank the Department of Mechanical Engineering, MVJ College of Engineering, Bengaluru, India, and the Department of Mechanical Engineering, CMR Institute of Technology, Bengaluru, India, for supporting to carry out this work.

References

- [1] S. R. Babu, S. Karthikeyan, P. Senthilkumar, and B. Koodalingam, "Mechanical behavior on tamarind & dates seeds powder, prawn shells powder with Arundo donax L. leaf reinforced epoxy composite," *Materials Today: Proceedings*, vol. 33, pp. 3031–3036, 2020.
- [2] D. Verma, K. L. Goh, and V. Vimal, "Interfacial studies of natural fiber-reinforced particulate thermoplastic composites and their mechanical properties," *Journal of Natural Fibers*, vol. 19, pp. 1–28, 2020.
- [3] T. Srinivasan, S. B. Kumar, G. Suresh et al., "Experimental investigation and fabrication of Palmyra palm natural fiber with tamarind seed powder reinforced composite," in *IOP Conference Series: Materials Science and Engineering*, vol. 988, p. 12022, IOP Publishing, 2020, No. 1.
- [4] G. U. Raju and S. Kumarappa, "Experimental study on mechanical properties of groundnut shell particle-reinforced epoxy composites," *Journal of Reinforced Plastics and Composites*, vol. 30, no. 12, pp. 1029–1037, 2011.
- [5] G. K. Chowdari, D. K. Prasad, and S. B. R. Devireddy, "Physical and thermal behaviour of areca and coconut shell powder

- reinforced epoxy composites,” *Materials Today: Proceedings*, vol. 26, pp. 1402–1405, 2020.
- [6] S. K. Saw, R. Purwar, S. Nandy, J. Ghose, and G. Sarkhel, “Fabrication, characterization, and evaluation of luffa cylindrical fiber reinforced epoxy composites,” *Bio Resources*, vol. 8, no. 4, pp. 4805–4826, 2013.
 - [7] S. Noone, K. Purushothaman, and R. Pradhan, “An investigation on luffa cylindrical fiber reinforced epoxy composite,” *Materials Today: Proceedings*, vol. 33, pp. 1026–1031, 2020.
 - [8] D. Sreeramulu and N. Ramesh, “Synthesis, characterization, and properties of epoxy filled Luffa cylindrica reinforced composites,” *Materials Today: Proceedings*, vol. 5, no. 2, pp. 6518–6524, 2018.
 - [9] B. Stalin, N. Nagaprasad, V. Vignesh et al., “Evaluation of mechanical, thermal and water absorption behaviors of polyalthia longifolia seed reinforced vinyl ester composites,” *Carbohydrate Polymers*, vol. 248, p. 116748, 2020.
 - [10] O. V. Potadar and G. S. Kadam, “Preparation and testing of composites using waste groundnut shells and coir fibres,” *Procedia Manufacturing*, vol. 20, pp. 91–96, 2018.
 - [11] R. Potluri, K. J. Paul, and P. Prasanthi, “Mechanical properties characterization of okra fiber based green composites & hybrid laminates,” *Materials Today: Proceedings*, vol. 4, no. 2, pp. 2893–2902, 2017.
 - [12] M. N. A. Marzuki, I. S. M. A. Tawakkal, M. S. M. Basri et al., “The effect of jackfruit skin powder and fiber bleaching treatment in PLA composites with incorporation of thymol,” *Polymers*, vol. 12, no. 11, p. 2622, 2020.
 - [13] V. S. Aigbodion and C. U. Atuanya, “Improving the properties of epoxy/melon shell bio-composites: effect weight percentage and form of melon shell particles,” *Polymer Bulletin*, vol. 73, no. 12, pp. 3305–3317, 2016.
 - [14] P. R. Sekaran, S. G. Kumar, J. A. J. Singh, and J. Vairamuthu, “Experiment investigation and analysis of fish scale reinforced polymer composite materials,” *Materials Today: Proceedings*, vol. 33, pp. 4542–4545, 2020.
 - [15] K. R. Babu, V. Jayakumar, G. Bharathiraja, and S. Madhu, “Experimental investigation of fish scale reinforced polymer composite,” *Materials Today: Proceedings*, vol. 22, pp. 416–418, 2020.
 - [16] T. M. Somashekhar, P. Naik, V. Nayak, and S. Rahul, “Study of mechanical properties of coconut shell powder and tamarind shell powder reinforced with epoxy composites,” in *IOP Conference Series: Materials Science and Engineering*, vol. 376, p. 12105, IOP Publishing, 2018.
 - [17] G. Ravichandran, G. Rathnakar, N. Santhosh, and R. Suresh, “Wear characterization of HNT filled glass-epoxy composites using Taguchi’s design of experiments and study of wear morphology,” *Composites Theory and Practice*, vol. 20, no. 2, pp. 85–91, 2020.
 - [18] B. A. Praveena, N. Santhosh, D. P. Archana et al., “Influence of nanoclay filler material on the tensile, flexural, impact, and morphological characteristics of jute/E-glass fiber-reinforced polyester-based hybrid composites: experimental, modeling, and optimization study,” *Journal of Nanomaterials*, vol. 2022, Article ID 1653449, 2022.
 - [19] N. Santhosh, B. A. Praveena, H. V. Srikanth et al., “Experimental investigations on static, dynamic, and morphological characteristics of bamboo fiber-reinforced polyester composites,” *International Journal of Polymer Science*, vol. 2022, Article ID 1916877, 2022.
 - [20] “Subhakanta Nayak, Mohanty, J. R. Optimization of operating parameters for abrasion of areca sheath reinforced polymer composite: grey based Taguchi approach,” *International Journal of Plastics Technology*, vol. 22, no. 1, pp. 26–40, 2018.
 - [21] B. A. Praveena, B. Abdulrajak, N. Santhosh, V. K. Kedambadi, H. Jaibheem, and D. Huliya, “Study on characterization of mechanical, thermal properties, machinability and biodegradability of natural fiber reinforced polymer composites and its applications, recent developments and future potentials: a comprehensive review,” *Material Today Proceedings*, vol. 52, Part 3, pp. 1255–1259, 2021.
 - [22] G. Anand, N. Santhosh, and S. Vishvanathperumal, “Introduction to aging in bio composites,” in *Aging Effects on Natural Fiber-Reinforced Polymer Composites, Composites Science and Technology*, C. Muthukumar, S. Krishnasamy, S. M. K. Thiagamani, and S. Siengchin, Eds., pp. 1–16, Springer, Singapore, 2022.
 - [23] B. A. Praveena, N. Santhosh, H. V. Abdulrajak Buradi et al., “Experimental investigation on density and volume fraction of void, and mechanical characteristics of areca nut leaf sheath fiber-reinforced polymer composites,” *International Journal of Polymer Science*, vol. 2022, Article ID 6445022, 2022.
 - [24] B. A. Praveena, S. Vijay Kumar, H. N. Manjunath et al., “Investigation of moisture absorption and mechanical properties of natural fiber reinforced polymer hybrid composite,” *Materials Today Proceedings*, vol. 45, Part 9, pp. 8219–8223, 2021.
 - [25] S. Nagaraja, P. Bindiganavile Anand, R. N. Mahadeva Naik, and S. Gunashekarana, “Effect of aging on the biopolymer composites: mechanisms, modes and characterization,” *Polymer Composites*, vol. 43, no. 5, pp. 1–11, 2022.
 - [26] G. Ravichandran, G. Rathnakar, N. Santhosh, R. Chennakeshava, and M. A. Hashmi, “Enhancement of mechanical properties of epoxy/halloysite nanotube (HNT) nanocomposites,” *SN Applied Sciences*, vol. 1, p. 296, 2019.
 - [27] G. Ravichandran, G. Rathnakar, N. Santhosh, and R. Suresh, “A comparative study on the effect of HNT and nano-alumina particles on the mechanical properties of vacuum bag moulded glass-epoxy nanocomposites, mechanics of advanced,” *Composite Structures*, vol. 8, pp. 119–131, 2021.
 - [28] G. Ravichandran, G. Rathnakar, and N. Santhosh, “Effect of heat treated HNT on physico-mechanical properties of epoxy nanocomposites,” *Composites Communications*, vol. 13, no. 2, pp. 42–46, 2019.
 - [29] N. P. Sunesh, “Isolation and characterization of novel agrowaste-based cellulosic micro fillers from *Borassus flabellifer* flower for polymer composite reinforcement,” *Polymer Composites*, vol. 43, no. 9, pp. 6476–6488, 2022.
 - [30] P. J. Herrera-Franco and A. Valadez-González, “Mechanical properties of continuous natural fibre-reinforced polymer composites, composites part A: applied science and manufacturing,” vol. 35, no. 3, pp. 339–345, 2004.
 - [31] V. Naik, M. Kumar, and V. Kaup, “Evaluation of flexural and impact behaviour of mango seed shell short fiber reinforced composites,” *Materials Today: Proceedings*, vol. 62, no. 8, pp. 5546–5549, 2022.
 - [32] A. M. Kazi, D. V. A. Ramasastry, S. Waddar, T. Mohamed, S. Shaikh, and A. A. Tamboli, “Water absorption and thickness swelling behaviour of woven roselle fibre epoxy composites,” *International Journal of Vehicle Structures & Systems*, vol. 14, no. 1, pp. 37–40, 2022.
 - [33] S. Sanjeevi, V. Shanmugam, S. Kumar et al., “Effects of water absorption on the mechanical properties of hybrid natural fibre/phenol formaldehyde composites,” *Scientific Reports*, vol. 11, no. 1, p. 13385, 2021.